

---

## Identifying parameters of equivalent circuit and simulating machining process in electrochemical machining with bipolar pulses and an auxiliary electrode

Qingrong Zhang <sup>1</sup>, Wataru Natsu <sup>1</sup>

<sup>1</sup>Tokyo University of Agriculture and Technology

[summer@go.tuat.ac.jp](mailto:summer@go.tuat.ac.jp)

---

### Abstract

The authors have proposed a novel electrochemical machining method that uses bipolar pulses and an auxiliary electrode (hereinafter referred to as BPAE-ECM) to deliberately generate a dense hydrogen bubble film on the side of the tool electrode and the non-machining surface of the workpiece, thereby increasing the electrical resistance that obstructs the flow of electrolytic current and achieving improved machining accuracy. The effectiveness of the proposed method was verified through simulations and experiments. However, owing to the change in the polarity of the workpiece in BPAE-ECM, the charging and discharging behavior of the EDL is affected, which influences the anodic Faradaic current used to remove the workpiece material and thus governs machining accuracy. The Faradaic current can be indirectly obtained with a simulation by constructing an equivalent circuit and identifying its parameter values. In this study, the parameters of the equivalent circuit for BPAE-ECM are experimentally identified based on the actual voltage and current waveforms obtained from machining experiments, and the effects of bipolar pulses and an auxiliary electrode are simulated based on the obtained parameters.

Keywords: electrochemical machining; equivalent circuit; parameter; bipolar pulses; auxiliary electrode

---

### 1. Introduction

Electrochemical machining (ECM) is a nonconventional processing method that utilizes electrochemical reactions to remove workpiece material. Although it has advantages of no tool wear and no mechanical cutting force, it has a fatal disadvantage of reduced machining accuracy due to unwanted stray corrosion. As effective methods for reducing stray corrosion in ECM, ultrashort pulse ECM [1], ECM with insulating films [2], and electrolyte confinement by absorption materials [3] have been proposed.

In our previous study, a novel electrochemical machining method that uses bipolar pulses and an auxiliary electrode (hereinafter referred to as BPAE-ECM) was proposed [4], in which intensive hydrogen bubbles are generated on the side of the tool electrode and the non-machining surface of the workpiece. The generated hydrogen bubbles are used to block the harmful stray current because of their good insulating properties, thereby improving machining accuracy by reducing stray corrosion. Meanwhile, the alteration of the workpiece polarity in BPAE-ECM influences the charging and discharging process of the electric double layer (EDL), which affects the material removal in different areas, thereby affecting the machining accuracy. One of the methods to elucidate the charging process of EDL is to construct and analyze an equivalent circuit by identifying the equivalent circuit parameters in BPAE-ECM.

The identification of equivalent circuit parameters is a complex task that usually requires expensive equipment, such as an electrochemical workstation. Several researchers have investigated the application of electrochemical

workstations for performing electrochemical impedance spectroscopy (EIS) tests to identify the equivalent circuit parameters in ECM. For example, Shen et al. [5] used EIS to identify these parameters, which were used to simulate the distribution of the Faradaic current density and material removal in ECM with an electrolyte suction tool. Sharma et al. [6] obtained the equivalent circuit parameters by fitting the values in the Nyquist plot in the EIS test, and used these parameters to construct an equivalent electrical circuit for simulating the Faradaic current in different waveforms of pulsed voltage. EIS can accurately identify the parameters of the ECM equivalent circuit; however, it is costly and time-consuming.

An alternative and more cost-effective method for identifying equivalent circuit parameters is to analyze the experimentally obtained voltage and current waveforms in our previous study [7]. On this basis, the authors used this method to identify the equivalent circuit parameters of the BPAE-ECM and simulate the effects of the bipolar pulses and auxiliary electrode based on the obtained parameters.

### 2. Equivalent Circuit Model of BPAE-ECM

It is well-known that in ECM, the total current through the metal/solution interface has two parts. The current flowing through the Faradaic resistance is called the Faradaic current, which is responsible for anodic dissolution. Another part that flows through and charges the EDL capacitance is called the capacitance current, which is not directly responsible for material dissolution. In BPAE-ECM, analyzing Faradaic currents in the machining and non-machining areas of the workpiece surface is effective to investigate the material

removal mechanism. However, since there is no instrument to directly measure the Faradaic current, the Faradaic current can only be indirectly obtained by calculating the ECM equivalent circuit.

The electrochemical system of BPAE-ECM includes a workpiece, tool, auxiliary electrode, electrolyte, and bipolar pulse power supply. Figure 1 shows the established equivalent circuit model of BPAE-ECM. This model includes EDL capacitances ( $C_{d1}, C_{d2}, C_{d3}, C_{d4}$ ), Faradaic resistances ( $R_{d1}, R_{d2}, R_{d3}, R_{d4}$ ), and electrolyte resistances ( $R_{e1}, R_{e2}, R_{e3}, R_{e4}$ ) in different areas. It should be pointed out that for simplicity, the EDL capacitance and Faradaic resistance at the surface of the auxiliary electrodes are ignored because the consumption of negative pulse current does not affect the ratio of negative pulse current flowing through the machining and non-machining areas.

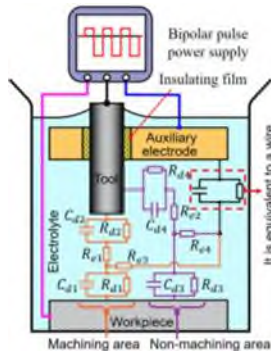


Figure 1. Equivalent circuit model of BPAE-ECM.

### 3. Method for identifying parameters

#### 3.1. Theoretical analysis

In this research, the equivalent circuit parameters are identified by analyzing experimentally obtained voltage and current waveforms. Figure 2 shows the process of identifying equivalent circuit parameters in two equal-sized areas of electrodes. As shown in Figure 2(c), at the moment when the power supply is turned on, the EDL capacitances ( $C_{dx}$  and  $C_{dy}$ ) behave as short circuits and start to be charged, which can be equivalent to shortening the Faradaic resistances ( $R_{dx}$  and  $R_{dy}$ ). The current is determined only by electrolyte resistance. Therefore, the electrolyte resistance ( $R_{ex}$ ) can be calculated by Equation (1).

$$R_{ex} = \frac{U_p}{I_1(t_1)} \quad (1)$$

where time  $t_1$  denotes the moment at which the EDL capacitances begin charging.

As shown in Figure 2(d), when the EDL capacitances are fully charged, the current stops changing during the subsequent pulse-on period. The equivalent circuit equates to the Faradaic resistances and electrolyte resistance in series, and the Faradaic resistance can be calculated by Equation (2).

$$R_{dx} = R_{dy} = 2 \left( \frac{U_p}{I_1(t_2)} - R_{ex} \right) \quad (2)$$

where time  $t_2$  is defined as the start point from which the current value ceases to change.

As shown in Figure 2(e), when the application voltage is stopped, the EDL capacitances begin to discharge. The current flows in this RC circuit can be calculated by Equations (3), (4), and (5).

$$I_1(t_4) = I_1(t_3)e^{-\frac{t_4-t_3}{RC_{dx}}} \quad (3)$$

$$R = \frac{R_{ex}R_{dx}}{2R_{dx} + R_{ex}} \quad (4)$$

$$\ln(I_1(t_4)) = \frac{t_4 - t_3}{RC_{dx}} + \ln(I_1(t_3)) \quad (5)$$

where  $t_3$  denotes the moment at which the capacitance begins to discharge, and  $t_4$  is defined as the discharge time, representing the point at which the reverse current amplitude reaches approximately 37% of the peak value of the reverse current in this study.

The slope ( $k$ ) of the line defined by Equation (5) can be used to approximate the EDL capacitances, which can be calculated by

$$C_{dc} = C_{dt} = \frac{1}{R * k} \quad (6)$$

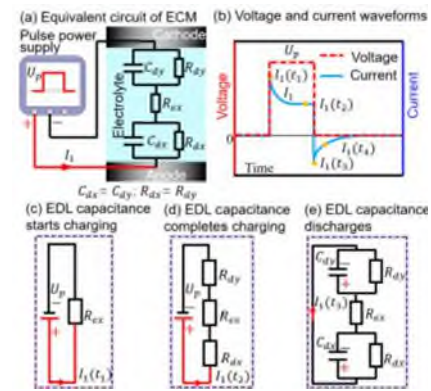


Figure 2. Process of identifying equivalent circuit parameters of ECM.

Based on the above calculation procedure, the equivalent circuit parameters of BPAE-ECM can be calculated.

#### 3.2. Identifying parameters by experiment and simulation

The experimental parameters are listed in Table 1, and used to identify the parameters of the equivalent circuit.

Table 1 Experimental parameters	
Parameters	Values
Positive pulse voltage, $U_p$	10 V
Negative pulse voltage, $U_p$	16 V
Positive pulse period, $t_p$	100 $\mu$ s
Negative pulse period, $t_p$	100 $\mu$ s
Workpiece	304 stainless steel
Tool	304 stainless steel
Electrolyte	NaNO <sub>3</sub> aq. 10 wt%
Inter-electrode gap (IEG)	100 $\mu$ m

Figure 3 shows the experimental and calculated current flow through the ECM equivalent circuit in machining and non-machining areas. As shown in Figure 3(a), insulating films were used to limit the electrochemical reaction area to a small area, and a single pulse voltage ( $U_p$ ) was applied to the workpiece and tool. The current ( $I_p$ ) passing through the workpiece surface is the sum of two currents: current ( $I_{p1}$ ) in the machining area and current ( $I_{p2}$ ) in the non-machining area. As shown in Figure 3(c), two electrode rods with the same diameter of 1 mm were placed into transparent glass maintaining a certain IEG of 100  $\mu$ m, and the electrolyte was filled, which is equivalent to restricting the electrochemical reaction between the machining area of the workpiece and the end face of the tool to obtain the current  $I_{p1}$  by applying

a pulse voltage (). To reduce the intensive noise in the current waveform, a low-pass filter with a cutoff frequency of 5 MHz was introduced. Therefore, the current  $(2)$  in the non-machining area was calculated from the filtered currents and  $1$ . It was assumed that the values of the EDL capacitance and Faradaic resistance in the non-machining area and tool sidewall are the same. The equivalent circuit parameters can be identified by analyzing the experimentally obtained current waveform of  $1$  and  $2$ .

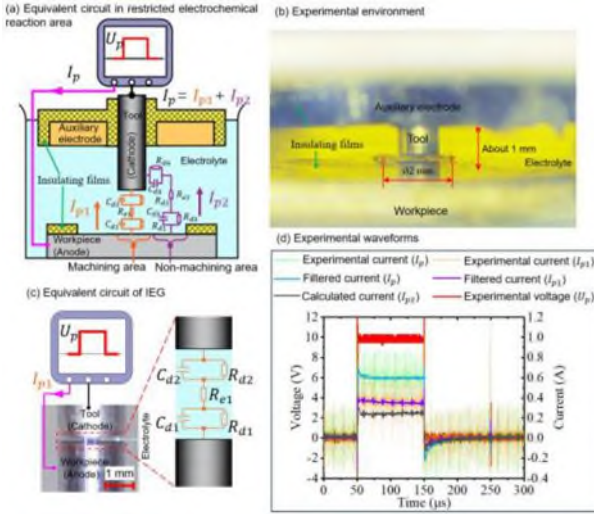


Figure 3. Current flow through the equivalent circuit of ECM.

Compared with conventional electrochemical machining with a unipolar pulse (UP-ECM), the charge of EDL on the workpiece surface is affected by the negative pulse current from the auxiliary electrode in BPAE-ECM. Therefore, it is necessary to calculate the equivalent electrolyte resistances between the auxiliary electrode and the different areas of the workpiece surface. To investigate the ratio of negative pulse currents flowing into the machining and non-machining areas in BPAE-ECM, as shown in Figure 4 (a), a 2D simulated model of an electric field was carried out, and the electrolyte with a conductivity of 10 S/m was designated as the simulated area. As shown in Figure 4(b), it is difficult for the negative pulse current to flow into the narrow IEG. As shown in Figure 4(c), the calculated average negative-pulse current density () in the machining area (at the position of 0-0.5 mm) of the workpiece surface is about 0.135 A/cm<sup>2</sup>, while this value () in the non-machining area (at the position of 0.5-1mm) is about 7.707 A/cm<sup>2</sup>.

The process of identifying equivalent electrolyte resistance between the auxiliary electrode and workpiece is based on the experimental environment shown the Figure 3(b). As shown in Figure 5, the workpiece and tool are set as the cathodes, while the auxiliary electrode is set as the anode, and a certain pulse voltage () was applied to obtain a current waveform () flowing into the workpiece. When the power supply was turned on to reach the peak current value, the current flows only through the electrolyte resistance. Based on the calculated average negative pulse current density in different areas of Figure 4(c), the values of the currents ( $3$  and  $4$ ) flowing through the machining and non-machining area can be approximated by Equations (7) and (8). Therefore, the equivalent electrolyte resistances ( $3$  and  $4$ ) can be calculated by Equation (9).

$$3 = \frac{(1) * (*)}{* + *} \quad (7)$$

$$4 = \frac{(1) * (*)}{* + *} \quad (8)$$

$$= \frac{(-3,4)}{(-3,4)} \quad (9)$$

where and are the size of machining and non-machining areas, respectively.

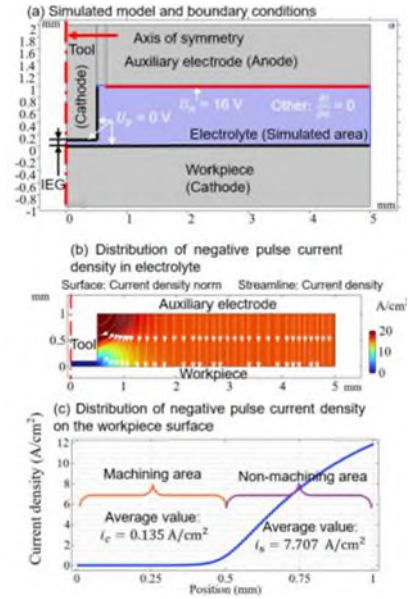


Figure 4. Simulation of the distribution of negative-pulse current density in BPAE-ECM.

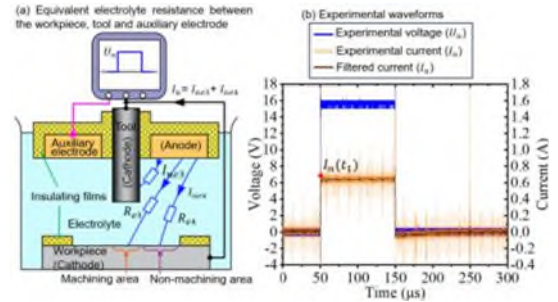


Figure 5. The equivalent circuit between auxiliary electrode and workpiece when the current reaches its peak value.

#### 4. Simulation of equivalent circuit of BPAE-ECM

Based on the above calculations and analysis, Table 1 lists the identified parameters of the equivalent circuit in BPAE-ECM. Figure 6 shows the equivalent circuit model of BPAE-ECM coupled with the principle enabling circuit of bipolar pulse power supply in the circuit simulation software Multisim.

Table 1 The values of each circuit element

Parameters	Corresponding values in sequence
$(= 1, 2, 3, 4)$	4.519 $\mu$ F, 4.519 $\mu$ F, 7.96 $\mu$ F, 7.96 $\mu$ F
$(= 1, 2, 3, 4)$	2.473 O, 2.473 O, 3.123 O, 3.123 O
$(= 1, 2, 3, 4)$	24.021 O, 33.09 O, 4103.432 O, 23.963 O

In addition, experiments with the same configuration as that shown in Figure 3(b) were necessary to verify the reliability of the identified parameters. Figure 7 shows the machining current waveforms flowing through the workpiece in both the experiment and simulation in UP-ECM and BPAE-ECM. Based on the degree of agreement between the experimental and simulated waveforms, it can be concluded



that the simulated results are relatively close to the experimental results. These results validate the reliability of the proposed calculation method.

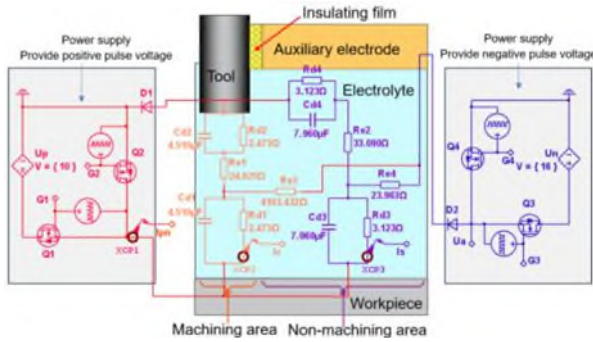


Figure 6. Principle-enabling circuit of the bipolar pulse power supply and the equivalent circuit model in BPAE-ECM.

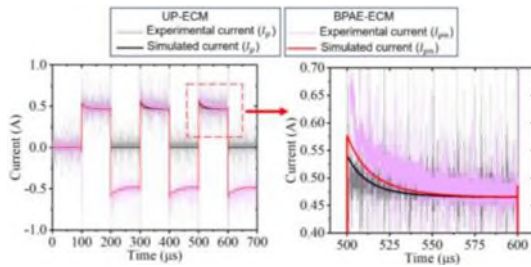


Figure 7. Machining current waveform in both the experiment and simulation in UP-ECM and BPAE-ECM.

Figure 8 shows the simulated Faradaic current. It can be observed that the Faradaic current in the machining area of BPAE-ECM is nearly the same as that of the UP-ECM. However, compared with UP-ECM during the positive pulse period, the Faradaic current in the non-machining area exhibits a reduction in both the peak value and duration time in BPAE-ECM. Therefore, the workpiece material dissolution is reduced in the non-machining area of the BPAE-ECM owing to the low anodic Faradaic current.

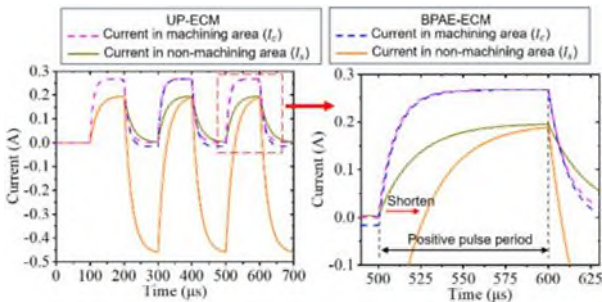


Figure 8. The Faradaic currents in the simulation.

To investigate the effect of Faradaic current in the non-machining area on material removal in BPAE-ECM, the same pulse voltage parameters utilized in the simulation were employed to analyze the differences in material removal between the two methods in experiments with stationary electrodes and static electrolyte. Figure 9 shows the holes machined by UP-ECM and BPAE-ECM after machining for 1 min. It can be observed that the hole machined by BPAE-ECM has higher precision with a smaller overcut and deeper depth than that machined by UP-ECM. Excluding the effect of hydrogen bubbles, these results indicate that the material removal in the non-machining area can be reduced due to the low anodic Faradaic current in BPAE-ECM.

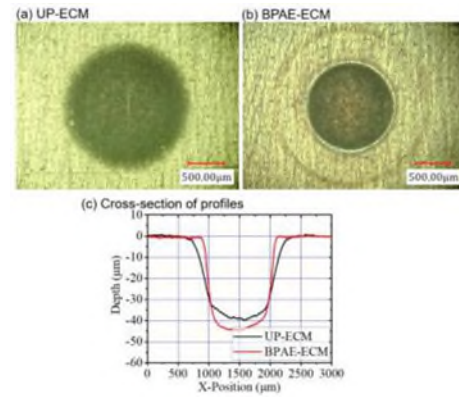


Figure 9. The holes machined by UP-ECM and BPAE-ECM.

## 5. Conclusions

In this study, the equivalent circuit of BPAE-ECM was established and its parameter values were identified to investigate the effect on bipolar pulse and auxiliary anodes. The following conclusions were obtained:

- (1) The equivalent circuit parameters can be identified by analyzing the experimentally obtained current waveforms. By comparing the overlap of simulated and experimental current waveforms, the reliability of the identified parameters was verified.
- (2) The simulated results showed that the application of bipolar pulses and an auxiliary electrode can reduce the Faradaic current in the non-machining area of the workpiece surface during the positive pulse period, which is beneficial for reducing the material removal in the non-machining area.

## Acknowledgement

This work was supported by The Precise Measurement Technology Promotion Foundation, Japan.

## References

- [1] R. Schuster, V. Kirchner, P. Allongue, G. Ertl, Electrochemical Micromachining, *Science* 289 (2000) 98–101.
- [2] L. Yong, H. Ruiqin, Micro Electrochemical Machining for Tapered Holes of Fuel Jet Nozzles, *Procedia CIRP* 6 (2013) 395–400. <https://doi.org/10.1016/j.procir.2013.03.085>.
- [3] J. Wang, W. Natsu, Stray-corrosion-free ECM with electrolyte absorbed in a porous solid ball for dimple texturing on finished workpiece surfaces, *J. Manuf. Process.* 85 (2023) 713–723.
- [4] Q. Zhang, W. Natsu, H. Luo, Realization of high-precision electrochemical machining by active use of hydrogen bubbles generated in non-machining area, *Precis. Eng.* 91 (2024) 59–76.
- [5] C. Shen, J. Wang, P. Zhou, Y. Yan, D. Guo, Multi-factor coupling analysis of electric field distribution in electrochemical machining with electrolyte suction tool, *Precis. Eng.* 89 (2024) 504–516.
- [6] V. Sharma, M. Gyanprakash D., P. Gupta, J. Ramkumar, Analysis of circuit current in electrochemical micromachining process under the application of different waveforms of pulsed voltage, *J. Manuf. Process.* 75 (2022) 110–124.
- [7] Q. Zhang, H. Luo, W. Natsu, Parameter Identification of Equivalent Circuit for Pulsed Electrochemical Machining Based on Experimentally Obtained Current Waveforms, *Int. J. Precis. Eng. Manuf.* 25 (2024) 2491–2500.